Results of the 1996 Earth Observing System vicarious calibration joint campaign at Lunar Lake Playa, Nevada (USA)

K. Thome, S. Schiller, J. Conel, K. Arai and S. Tsuchida

Abstract. A joint campaign was held at Lunar Lake Playa, Nevada (USA) in June 1996 to evaluate the accuracy of reflectance-based, vicarious calibrations of Earth Observing Systems (EOS). Four groups participated in the campaign and made independent measurements of surface reflectance and atmospheric transmittance on five different days. Each group predicted top-of-the-atmosphere radiance for several bands in the 400 nm to 2500 nm spectral range. Analysis of the data showed differences of the order of 5% to 10% throughout the spectral region under study. Further study revealed that the major sources of discrepancy are differences in procedures and assumptions in finding the reflectance of field references used to determine the surface reflectance of the test site. Differences caused by varying radiative transfer codes and aerosol assumptions were found to be a relatively small error source, owing to the high reflectance and low turbidity of the test site. Differences in the solar irradiance values used by separate groups were found to be significant, but can be overcome by agreeing on a standard solar irradiance data set. The results from this campaign were used to plan a follow-up campaign in June 1997 that included developing a set of laboratory measurements to characterize the field radiometers which measure surface reflectance, and obtaining a consistent set of reference-panel reflectance factors. The expectation is that disagreement in absolute radiances at the top of the atmosphere generated by these field methods will be reduced to less than 3% if further cooperative work between groups is carried out to develop approaches which will account better for reference panel calibration, the consistent use of atmospheric characterization and radiative transfer codes.

1. Introduction

This paper summarizes the results of a field campaign held at Lunar Lake Playa, Nevada (USA) from 30 May to 4 June 1996. The campaign was a joint experiment to examine the accuracy of vicarious calibration for several EOS sensors. Representatives from the science teams of the sensors ASTER (Advanced Spaceborne Thermal Emission and Reflection Radiometer), MISR (Multi-angle Imaging Spectroradiometer), and MODIS (Moderate-resolution Imaging Spectroradiometer), as well as a representative from South Dakota State University (SDSU) took part in the experiment.

K. Thome: Optical Sciences Center, University of Arizona, PO Box 210094, Tucson, AZ 85721-0094, USA.
S. Schiller: Physics Department, South Dakota State University, Box 2219, Brookings, SD 57007, USA.
J. Conel: Jet Propulsion Laboratory, M/S 169-237, 4800 Oak Grove Dr., Pasadena, CA 91109-8099, USA.
K. Arai: Department of Information Science, Saga University, 1 Honjo, Saga 840, Japan.
S. Tsuchida: Environmental Geology Department, GSJ, Higashi 1-1-3, Tsukuba, Ibaraki 305, Japan.

The group representing MISR came from the Jet Propulsion Laboratory and is referred to as the MISR group. There were two groups representing ASTER in the visible and near-infrared (VNIR) and the short-wave infrared (SWIR), one from the Japanese ASTER Calibration team (JAC) and the other from the Remote Sensing Group of the Optical Sciences Center at the University of Arizona (UA). The UA group also represented MODIS.

Measurements were made in the VNIR, SWIR, and thermal infrared portions of the spectrum. This paper, however, presents only the results of the work done in the VNIR and SWIR.

Vicarious calibration refers to methods of in-flight calibration that are independent of on-board calibrators. They are a critical aspect of calibrations for NASA's Earth Science project [1], one of the goals of which is to create long-term, absolutely calibrated sets of observations for the study of global change. The project will use multiple sensors on various platforms, with a calibration team for each sensor. Most of the sensor teams use some form of vicarious calibration in their work. Thus, it is essential to ensure that different groups

Metrologia, 1998, 35, 631-638

performing these calibrations obtain consistent results to prevent biases between different sensors.

The specific method of vicarious calibration discussed here is the reflectance-based approach developed in the late 1980s for the radiometric calibration of Landsat-4 and Landsat-5 Thematic Mappers [2]. The method has been successfully applied to several satellite [3-5] and airborne sensors [6, 7]. The method relies on measuring the surface reflectance, atmospheric optical thicknesses, and aerosol properties at a test site at the time of a sensor overpass. The results of the measurements are used to constrain a radiative transfer code to predict a normalized radiance at the sensor that is converted to absolute radiances via an assumed solar spectral irradiance. The atmospheric measurements usually rely on solar extinction measurements, and these data are then converted to spectral optical depths that are used to describe aerosol parameters and columnar amounts of gaseous absorbers [8-12]. Surface reflectance data typically consist of the upwelling signal from the test site ratioed to data collected while viewing a panel of known reflectance to obtain the hemispherical-directional reflectance of the site [13].

Past work has shown that the expected uncertainties from the reflectance-based approach are less than 5 % for regions in the VNIR not affected by strong absorption [14], and that the primary contributions to the uncertainty are the uncertainties in aerosol refractive index and size distribution. Uncertainty in the surface reflectance is also a significant source of error. In fact, for the ideal atmospheric conditions sought for these experiments, namely low aerosol loading, the reflectance dominates the error budget in the predicted radiances at the top of the atmosphere. Biggar et al. [14] show that reasonable improvements in equipment and data collection methods should bring the total uncertainty to less than 3.5 %. For the SWIR, uncertainties are larger, owing to poorer knowledge of the reflectance standards, stronger gaseous absorption, and lower solar irradiance. On the other hand, aerosol effects in the SWIR are much smaller for typical test sites and this factor decreases the uncertainty in the atmospheric characterization.

In this work we present the reflectance-based results from the joint vicarious campaign held in June 1996. We first describe the test site used and how the data were collected. The predicted, normalized radiances at the top of the atmosphere for one of the data collections are then presented followed by discussions of the differences seen and the sources of these differences. The final section gives recommendations for future measurement campaigns.

2. Site and experiment description

Ideal sites for the reflectance-based approach present high reflectance and are located in regions of low aerosol loading to reduce uncertainties caused by atmospheric effects and to allow the sensor to be calibrated at a high radiance level. The area used for the calibration should ideally be located in the centre of a large, spatially homogeneous region (for example, White Sands Missile Range is approximately 2500 km^2) to reduce atmospheric adjacency effects and to sample a large number of detectors for pushbroom systems. The spectral reflectance of an ideal site is flat in order to reduce effects arising from changes in the spectral response of the system being calibrated. The test site selected for this work, Lunar Lake Playa in south-central Nevada, presents some of these qualities. As shown in Figure 1, the spectral reflectance is relatively flat and has a high value beyond 0.7 μm. This curve shows the difficulties of finding a site with uniformly flat spectral reflectance because the area suffers from the presence of iron (Fe^{+3}) absorption in the visible part of the spectrum, typical of playas in this region of the United States. The site is also spatially uniform, with portions of the playa varying by less than 0.5 % in reflectance over an area of 10^4 m^2. This playa measures approximately 3 km × 5 km, which is smaller than the ideal case, but the surface of the playa is hard and resistant to change from pedestrian and vehicular traffic. This made the site suitable for an experiment of this type, since we knew we would be walking on the target collecting data for several days with multiple collections each day. The primary site used for the work described here was a 240 m × 240 m area representative of the playa, assumed to approximate sixty-four 30 m × 30 m pixels. This area was located at approximately 38°23′ N. and 115°59′ W., and was laid out in a north-south/east-west orientation. In addition, three other Tracor radiometric calibration targets were used with essentially flat spectral reflectances of 2 %, 8 %, and 48 %. These targets were used for comparisons of surface reflectance retrievals.

The fieldwork consisted of several data collections per day for several days with measurements at

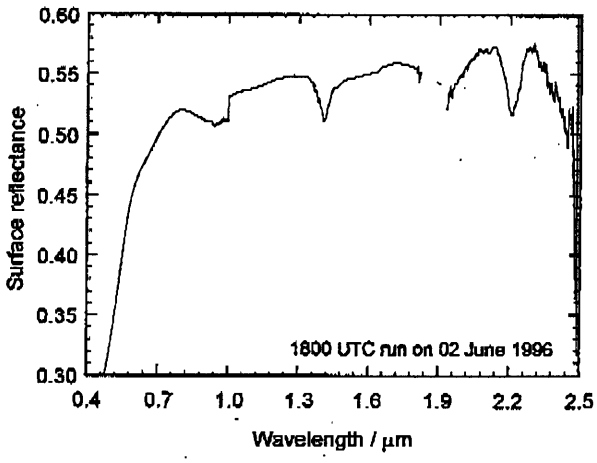

Figure 1. Spectral reflectance of the Lunar Lake Playa test site.

1420 UTC, 1600 UTC, 1800 UTC and 2120 UTC. The latter two times had similar solar zenith angles, and the 1800 time corresponded approximately to the time of the EOS-AM1 platform overpass. The 1420 and 1600 times had solar zeniths similar to what would be expected at the site at the time of AM-1 platform overpass at the winter solstice and the vernal and autumnal equinoxes.

All of the groups used essentially the same basic approach for collecting surface reflectance data. A radiometer was transported across the target and upwelling radiance was recorded. These radiances were compared with those measured from a reference of known reflectance to determine the reflectance of each sample point. Each group except the UA used Spectralon® as the reference standard; the UA group used an aluminium sheet painted with barium sulphate. The sizes of the references varied from the 61 cm × 61 cm (24″ × 24″) monolithic panel of the UA, to the 20.3 cm (8″) panels of the JAC and MISR groups. The SDSU measurements relied on a two-piece composite to create an approximately 45.7 cm × 45.7 cm (18″ × 18″) panel. The instruments used by each group consisted of Analytical Spectral Devices spectrometers. The JAC group used a PS-II spectrometer while the other three groups had FieldSpec FRs. The UA group also collected data using an eight-band Barnes MMR.

While the basic measurements of the surface reflectance were similar, the approaches to sampling the playa site spatially varied somewhat from group to group. The MISR group laid out a grid of 64 pixels and then randomly selected a single spot within each pixel and collected spectra. The other three groups walked in an east-west direction through the centre of each of the 64 pixels. The SDSU and Japanese teams collected point samples along this path, while the UA group sampled data in a continuous fashion.

Atmospheric measurements were made primarily by using solar radiometers constructed in the Electrical and Computing Engineering Department at the University of Arizona. The SDSU and MISR groups used automated versions of these solar radiometers while the UA group operated a manual version. The JAC group used a radiometer developed at the Meteorological Research Institute in Japan. In addition, the JAC group retrieved atmospheric parameters from measurements of skylight polarization. The SDSU and MISR groups also collected measurements of downwelling global and diffuse irradiance using multi-filter, shadow-band radiometers (MFRSRs) manufactured by Yankee Environmental Systems.

In addition to the reflectance and atmospheric data, each group collected ancillary data to indicate the quality of the data sets. These data included downwelling, directional sky radiance, temperature, relative humidity, and pressure. Also collected were pyranometer data to give an indication of the total downwelling irradiance as a function of time. Figures 2 and 3 show two examples of pyranometer data along with the times of the data collections made on each day. For example, on 1 June, the skies early in the day were clear, but the fluctuations later in the afternoon indicate that sky conditions were not as good, with more extensive cloud cover. The curve from 2 June, on the other hand, is much smoother for the entire day, indicating clear skies throughout the day. These curves show the difficulty with experiments of this type, since cloudy conditions greatly increase the uncertainty of reflectance-based results due to variations in the downwelling direct and diffuse irradiances. In order to simplify comparisons of the results, the goal of this campaign was thus to work in cloudless conditions. Of all the days, 2 June was the best in terms of sky conditions.

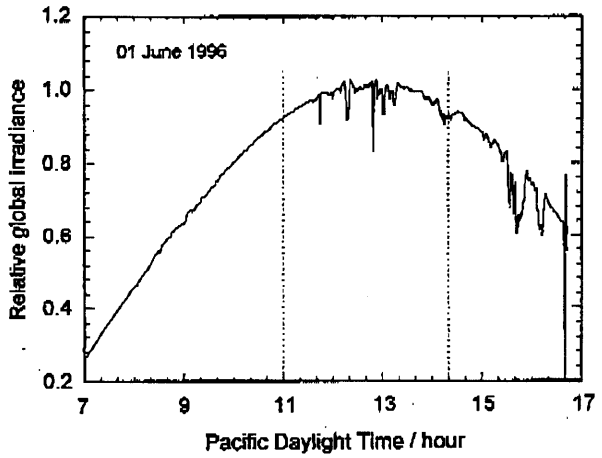

Figure 2. Plot of global irradiance from 1 June derived from pyranometer data. Overpass times are indicated by dotted lines.

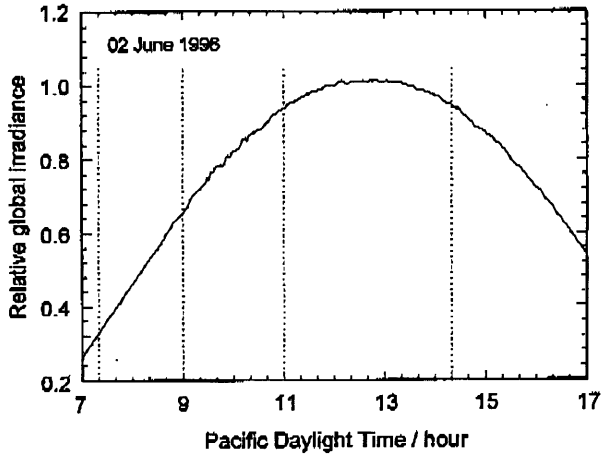

Figure 3. Plot of global irradiance from 2 June derived from pyranometer data. Overpass times are indicated by dotted lines.

3. Normalized radiance comparison

For comparisons of predicted radiances, it was decided to concentrate on the data set from 1800 UTC on 2 June because of the lack of clouds. The normalized-radiance results are shown in Table 1. We used normalized radiances here to avoid differences in assumed values for the exo-atmospheric solar irradiance. The results are for a set of "monochromatic" wavelengths at 450 nm, 550 nm, 650 nm, 800 nm, 1000 nm, 1600 nm and 2200 nm, as well as a set of six rectangular bands with centre wavelengths at 399 nm, 562 nm, 812 nm, 1027 nm, 1688 nm and 2217 nm and bandwidths of 10 nm, 100 nm, 100 nm, 10 nm, 100 nm and 100 nm, respectively. These wavelengths and bands sample the solar reflective portion of the spectrum while avoiding regions of strong atmospheric absorption. The JAC results are reported only for the VNIR because their spectrometer covering the short-wave infrared did not operate after shipment to the United States. The results indicate that the UA results are slightly higher than those of the other groups and this difference is larger at longer wavelengths. There is also a trend towards the results of the JAC group, with differences becoming larger with wavelength. These results are similar to those for other days and times. The causes of the differences are discussed here in terms of the retrieved surface reflectance, the atmospheric characterization, and the radiative transfer codes.

Table 1. Predicted normalized radiances at the top of the atmosphere over the Lunar Lake Playa target at 1800 UTC on 2 June 1996.

Central wavelength/μm	Normalized radiance			
	MISR	JAC	SDSU	UA
Rectangular bands				
0.399	0.0784	0.0766	0.0730	0.0792
0.562	0.1069	0.1040	0.1005	0.1112
0.812	0.1384	0.1260	0.1309	0.1367
1.027	0.1391		0.1379	0.1495
1.688	0.1371		0.1344	0.1393
2.217	0.1157		0.1127	0.1167
Monochromatic values				
0.450	0.0855	0.0848	0.0805	0.0876
0.550	0.1041	0.1025	0.0992	0.1090
0.650	0.1249	0.1193	0.1211	0.1287
0.800	0.1383	0.1332	0.1366	0.1440
1.000	0.1362		0.1378	0.1431
1.600	0.1379		0.1315	0.1342
2.200	0.1161		0.1121	0.1108

3.1 Surface reflectance

Cursory examination of the results revealed that a significant source of difference seen in the normalized radiances are differences in retrieved surface reflectance. Table 2 gives the retrieved reflectances used to derive the results in Table 1. Two sets of results from the UA group are shown in this table, with one set based on FieldSpec FR data and the other on MMR data. Figure 4 shows the percentage difference between the MISR retrieved reflectances for the monochromatic wavelengths and those of the UA FR data relative to the UA results, along with the percentage difference between the predicted at-sensor radiances of the two groups from Table 1. The correlation between the differences is expected because the high surface reflectance and low turbidity mean that the at-sensor radiance is dominated by the reflected radiance from the surface.

Past work by the UA has estimated that the uncertainty of its surface reflectance retrieval for a site such as Lunar Lake is 2%, or 0.01 in reflectance,

Table 2. Measured reflectances of the playa site used to determine predicted, normalized radiances at the top of the atmosphere at 1800 UTC on 2 June 1996.

Central wavelength/μm	Reflectance				
	MISR	JAC	SDSU	UA FR	UA MMR
Rectangular bands					
0.399	0.205	0.205	0.207	0.218	0.200
0.562	0.393	0.398	0.389	0.410	0.412
0.812	0.488	0.481	0.491	0.519	0.517
1.027	0.489		0.497	0.530	0.525
1.688	0.482		0.492	0.512	0.513
2.217	0.407		0.425	0.441	0.459
Monochromatic values					
0.450	0.266	0.274	0.268	0.282	0.270
0.550	0.375	0.386	0.378	0.397	0.402
0.650	0.453	0.454	0.452	0.478	0.479
0.800	0.488	0.485	0.491	0.521	0.516
1.000	0.479		0.494	0.510	0.525
1.600	0.486		0.492	0.517	0.516
2.200	0.411		0.418	0.429	0.485

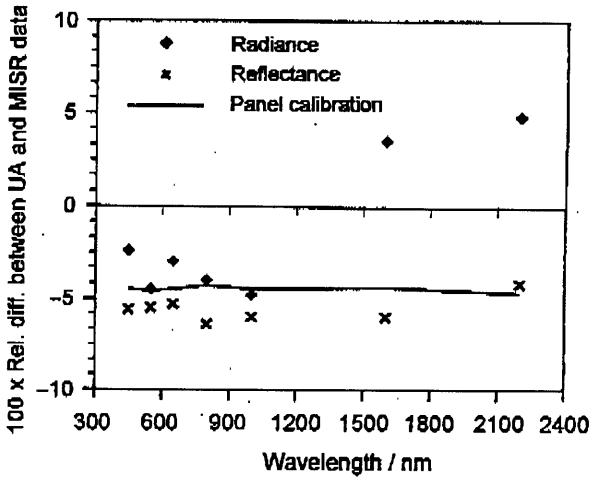

Figure 4. Percentage differences between MISR and UA reflectances and normalized radiances for the seven monochromatic bands. Also shown is the percentage difference between a hemispheric-directional and BRF calibration of a field reference.

at a reflectance of 0.5 [14]. This same work has also shown that for high-reflectance targets, the uncertainty in the at-sensor radiance results from and is roughly the same as the uncertainty in the reflectance. That is, a 2% uncertainty in reflectance leads to approximately 2% uncertainty in at-sensor radiance.

While the agreement in reflectance between the groups is quite satisfactory, the between-group differences are larger than what would be expected with this level of uncertainty. Possible sources for these larger-than-expected differences are the different samplings of the playa, types of panels used, methods for calibrating the field standard of reflectance, and use of panel bidirectional effects in the processing.

The first item was not a primary cause of the differences, since there was good agreement between the two UA instruments which were operated independently. In addition, the standard deviation of the average of 700 spectra from the UA's ASD FR collected over the entire 64-pixel site was less than 1.5% for all spectral ranges not affected by absorption. This is a good indication of the level of uniformity of the target.

The composition of the panels was not a major source of difference, but the manner in which these reference panels were calibrated and how the calibration was used caused differences. The method used by the UA was different from the other three since the UA group measured the bidirectional reflectance factor (BRF) of the field reference before and after each field campaign. The reflectance of each playa sample was determined by computing the BRF of the reference panel for the solar geometry of the measurement based on the time of the measurement. This method proved advantageous both in accounting for changes in the panel reflectance as a function of the solar incidence angle, and in correcting for the angle of incidence of the solar beam by the usual cosine factor. The other three groups used the spectral reflectance of their reference as determined from the hemispheric-directional reflectance factor (HRF) rather than the BRF. Their approaches did not include changes in the HRF caused by the changing solar zenith angle, nor was there a correction for the cosine of the solar zenith angle. For the MISR group, this cosine correction was not important since the reference panel and playa measurements were collected within one minute of each other. For the JAC and SDSU groups, the time lapse between panel and site measurements caused a change of up to 1%.

Two tests were carried out to examine the effect of using the HRF rather than the BRF. The first test involved a determination of the reflectance of the UA's barium sulphate reference at the monochromatic wavelengths using measurements performed by the SDSU group. The results of this comparison are shown in Table 3, with differences from 6% to 8%; smaller differences occurred at longer wavelengths. The second test consisted of processing data collected by the UA group with a monolithic Spectralon® panel using both the HRF and the BRF. The percentage differences between these results are shown by the solid line in Figure 4. The near coincidence of this line with the corresponding data for the UA and MISR reflectances indicates that much of the difference between the two groups can be attributed to the use of the BRF by the UA group and the HRF by the MISR group.

Table 3. Reflectances of the UA's barium sulphate reference measured at 1620 UTC on 3 June by the SDSU group and those derived from laboratory measurements by the UA group.

Wavelength/μm	Reflectance	
	SDSU	UA
0.450	0.873	0.943
0.550	0.883	0.952
0.650	0.881	0.953
0.800	0.871	0.945
1.000	0.843	0.926
1.600	0.772	0.826
2.200	0.655	0.695

The difficult question is whether to use HRF or BRF. In practice, neither is strictly correct, because there is a significant diffuse component from the sky that prevents the situation from being truly bi-directional. This is especially true in the "blue" bands of ASTER, ETM+, MISR, and MODIS where the diffuse skylight accounts for up to 10% of the reflected signal for the data shown here. The strong directional component from the Sun and the sky radiance as a function of zenith and azimuth angle make it complicated to treat the problem as hemispherical-directional. A parasol may be used to shade the panel and playa while collecting measurements to create a set of bidirectional data, but this method is unwieldy on a large scale and does not truly simulate the "reflectance" seen by the satellite, which includes the hemispherical component due to skylight. Collaborative efforts are currently under way between the four groups from this campaign, in addition to others, to decide which approaches may best be used for the determination of surface reflectance.

3.2 Atmospheric characterization

An additional source of the differences in the measured radiance are the atmospheric characterizations. One specific cause is the difference in aerosol optical depth for each of the bands. Table 4 shows the aerosol optical depths that each group used for determining the radiances for the monochromatic wavelengths in Table 1. From Table 4, it can be seen that most of the differences are around 0.01 except for the values from JAC. The differences also indicate that there are biases between the groups. That is, the MISR group has the lowest values at all wavelengths and the JAC group

Table 4. Aerosol optical depths used to predict normalized radiances at the top of the atmosphere over the Lunar Lake Playa target at 1800 UTC on 2 June 1996 for the seven monochromatic wavelengths.

Wavelength/μm	Optical depth			
	MISR	JAC	SDSU	UA
0.450	0.1035	0.1678	0.1132	0.1164
0.550	0.0749	0.1260	0.0839	0.0905
0.650	0.0572	0.0992	0.0655	0.0734
0.800	0.0410	0.0737	0.0480	0.0565
1.000	0.0286	0.0536	0.0345	0.0427
1.600	0.0134	0.0274	0.0171	0.0237
2.200	0.0080	0.0174	0.0106	0.0159

the highest. While all groups used Langley approaches to calibrate their solar radiometers, the data sets used by each group were for different days, different time periods, and different sampling intervals. Thus, it is likely that the calibrations of the solar radiometers resulted in the observed biases. To examine the effect of the differences in optical depth, the UA's radiative transfer code was run using all of the UA inputs, except that the aerosol optical depths were replaced by those of the other three groups. The results showed that the differences in the at-sensor radiance as a result of optical depth differences are less than 0.6 %.

A similar approach was used to determine the aerosol size distribution. Junge parameters were derived from the results of all of the groups and these were input to the UA radiative transfer code using the original UA inputs for all other parameters. The Junge parameters derived for each of the groups are given in Table 5 as are the predicted at-sensor radiances for each of the monochromatic wavelengths. The largest observed difference is only 0.7 %.

These two comparisons were somewhat contrived because the Junge parameter and aerosol optical depths are not independent inputs. A better comparison would use the Junge parameter and aerosol optical depths from each group in the same radiative transfer code to observe the effects of the aerosol parameterization.

Table 5. Junge parameters and normalized radiances at the top of the atmosphere over the playa target at 1800 UTC on 2 June 1996 for the seven monochromatic wavelengths. Radiances were generated with the UA radiative transfer code and the given Junge parameters.

Wavelength/μm	Normalized radiance			
	MISR	JAC	SDSU	UA
0.450	0.0867	0.0871	0.0870	0.0872
0.550	0.1085	0.1090	0.1088	0.1092
0.650	0.1303	0.1309	0.1307	0.1312
0.800	0.1461	0.1467	0.1465	0.1470
1.000	0.1437	0.1442	0.1441	0.1446
1.600	0.1548	0.1553	0.1552	0.1555
2.200	0.1464	0.1468	0.1467	0.1470
Junge parameter	3.611	3.429	3.488	3.255

The results of this test showed that the differences in characterizing the aerosol results are less than 0.5 % of the predicted normalized radiance.

An additional atmospheric factor to be considered is gaseous absorption. The groups corrected for this effect by computing the transmittance for the path from the Sun to the ground and from the ground to the sensor and by multiplying the radiative transfer code resulting from this transmittance. The transmittance was determined by using columnar water vapour and ozone amounts based on retrievals from solar extinction measurements [9-12]. The columnar water vapour value derived for the 1800 UTC data collection on 2 June by the UA was 0.96 cm and the columnar ozone was 0.239 cm-atm. Using these columnar amounts of absorbing gases leads to water vapour transmittances of 0.95 and 0.93 for the 1688 nm and 2217 nm bands, respectively, and a 0.93 transmittance for the 812 nm band. Water vapour transmittances in the other bands are close to unity. Ozone transmittance was 0.97 in the 562 nm band and 1.0 for the other bands. The uncertainty effects in the gaseous transmittance would be most noticeable for the 562 nm, 812 nm, 1688 nm and 2217 nm bands, but should still remain small since even the absence of absorption would change the results by a maximum of only 7 %. For monochromatic bands, differences in gaseous transmittance are more noticeable since monochromatic absorption is not a realistic situation. This factor is the most likely cause of the differences in radiance shown in Figure 4 for the SWIR bands that do not follow the trend of the reflectance data.

3.3 Radiative transfer codes

The third source of difference examined was the effect of the radiative transfer codes. Ideally, a methodical comparison of all of the codes used for this work should be carried out. However, it is still possible to obtain an idea of the expected effect from using different radiative transfer codes by comparing the results obtained from one radiative transfer code with respect to results reported by each group. For this, the monochromatic bands at 450 nm and 1000 nm were selected because gaseous absorption effects are negligible for these two bands. These two bands also give cases of high and low scattering optical depths.

The UA code was run using the inputs from the JAC, MISR, and SDSU groups. The aerosols were assumed to have a real index of refraction of 1.44 and an imaginary component of 0.005. The results are shown in Table 6. The differences between the Japan and UA codes do not appear significant for the one band shown and indicate that the 1 % stated uncertainty for the Gauss-Seidel code is reasonable. This 1 % uncertainty appears too small for the SDSU and JPL cases at the shorter wavelength. Differences in the codes would be larger for the shorter wavelength because of the larger

Table 6. Predicted normalized radiances at the top of the atmosphere over the Lunar Lake Playa target at 1800 UTC on 2 June 1996, computed by the UA Gauss-Seidel code.

Group	Predicted normalized radiance		
	Original	Gauss-Seidel	% difference
0.450 μm			
MISR	0.0855	0.0833	−2.6
JAC	0.0838	0.0831	−0.8
SDSU	0.0805	0.0840	4.3
1.000 μm			
MISR	0.1362	0.1351	−0.8
SDSU	0.1378	0.1393	1.1

dominance of scattering at this wavelength. The good agreement at the longer wavelength, however, indicates that when care is taken to ensure that the aerosol index of refraction and aerosol phase functions are handled consistently between groups, the radiative transfer codes are not a significant source of difference in vicarious calibration. This is especially true when one considers that vicarious calibration is usually carried out over bright targets with low aerosol loading. The differences between the UA and SDSU codes are significant enough to warrant further investigation, and more comparisons are planned to study the cause of these differences.

4. Exo-atmospheric solar irradiance

In order to convert the relative radiances from the radiative transfer codes to absolute radiances, an incident solar irradiance is required. Table 7 shows the band-averaged solar irradiances used by three of the groups. The values from the MISR group were derived from the World Radiation Center. The other two sets of values shown in the table were all derived in some fashion from MODTRAN3. The SDSU results also depend on the solar irradiance curve in MODTRAN3.

Table 7. Top-of-the-atmosphere solar irradiances used to convert the relative radiances to absolute values.

Central wavelength/μm	Exo-atmospheric solar irradiance (W/m²/μm)		
	MISR	JAC	UA
Rectangular bands			
0.399	1555	1360	1396
0.562	1789	1780	1792
0.812	1089	1073	1067
1.027	688	680	675
1.688	213	205	204
2.217	70.0	77.6	78.0
Monochromatic values			
0.450	2032	1995	2029
0.550	1828	1807	1847
0.650	1542	1467	1506
0.800	1108	1091	1088
1.000	723	726	713
1.600	240	246	214
2.200	75.8	80.4	80.4

Most of the differences are in the 0.5 % to 2 % range but there are still several values that differ by as much as 10 %. These differences are easy to correct by simply agreeing upon one single set of values to use. However, eliminating other values only improves the precision of the results and the uncertainty in the solar irradiance must be included in any error budget for work of this nature.

5. Conclusions and recommendations for collecting data in the future

The differences in the at-sensor radiances computed from the several sets of data collected at Lunar Lake Playa were larger than had been expected. Most of these differences can be attributed to the methods used by each group to determine the reflectance of their field references. The UA group used measurements of the BRF of their reference to determine the reflectance of the test site, while the others used HRF. Comparisons of the HRF calibration for one reference to the BRF indicate that this can cause up to a 5 % difference in the retrieved surface reflectance of the test site. Additional sources of differences, such as aerosol optical thickness, size distribution, and gaseous transmittance were found not to be important for this work. This agrees well with past sensitivity analysis studies for the reflectance-based approach. It should be pointed out that the sensitivity to size distribution may be misleading, since for the study shown here all of the groups used similar assumptions for the size distribution. This implies that there is high precision of the results, but no real conclusion about the uncertainty resulting from the aerosol size distribution can be made. All four groups are in the process of modifying, or have already modified, their aerosol retrievals to include diffuse/direct irradiance measurements and sky radiance: this will allow them to take into account differing aerosol size distributions. Better evaluations of the accuracy of the aerosol retrievals in subsequent field campaigns should result, along with experimental determinations of the aerosol index of refraction that at present may be a source of significant error.

Two final sources of differences were the radiative transfer codes used and the solar irradiance needed to convert from relative to absolute radiances. The radiative transfer code results imply that the codes are not a significant source of uncertainty when all of the codes are used in a similar fashion with similar assumptions and consistent inputs. This is not a trivial requirement, however, since many of the radiative transfer codes use disparate definitions for aerosol size distribution, limits on the aerosol sizes, and index of refraction. There are plans, however, to attempt a better understanding of these issues in future work. The solar irradiance values were also found to give significant differences in the predicted at-sensor radiances. These may be eliminated by selecting one consistent set

of values, but this approach may improve only the precision of the results and not the accuracy. It is crucial for the success of vicarious calibration to establish an accurate solar irradiance curve.

In addition to analysing the differences in predicted radiances from the reflectance-based approach, this field campaign also provided directions for planning future campaigns of this type. A second joint campaign was held at Lunar Lake in June 1997. Based on the results presented here, this second campaign focused on understanding the surface reflectance data arising from differences in instrumentation, data collection techniques, reference panel calibration, and use of reference panel calibrations in data processing. Emphasis was placed on collecting several coordinated surface reflectance data sets rather than collecting several coordinated full data sets. The targets for these data sets included a small playa surface in addition to the three reflectance targets mentioned in the second section of this paper. The small size of the targets allowed the surfaces to be oversampled by each group and reduced uncertainties from spatial nonhomogeneity and temporal effects.

A similar effort was made to analyse the reference panels used by each group. All of the reference panels were investigated by the UA group's facility to determine their BRF. In addition, laboratory data were collected to evaluate the responsivity of the field radiometers used to collect surface reflectance data. The results of these laboratory measurements will allow multiple-processing paths to determine the biases from the reference panel calibrations and how they are used to convert to reflectance. These biases will be studied by taking a single reflectance data set and having each group process the data to reflectance. Also, a single data set will be processed using multiple field references to convert to reflectance.

The final improvement included by the second campaign was the use of coordinated data collections that coincided with the flight of several satellite and airborne sensors overhead, including the Airborne Visible and Infrared Spectrometer (AVIRIS) and the MODIS Airborne Simulator. This improvement should allow us to evaluate better the status of the accuracies of the reflectance-based calibration. Preliminary processing of the data from this campaign has been completed, and reprocessing of the data using multiple-processing schemes and different reference panels is under way. The preliminary results indicate that a better understanding of the vicarious calibration has been achieved; the next step is to translate this understanding into more accurate results.

Acknowledgements. The authors would like to thank the many individuals who assisted in the data collection and processing. K. Thome's work was supported under NASA Contract NAS5-31717. The work carried out by the Jet Propulsion Laboratory, California Institute of Technology, is under contract with the National Aeronautics and Space Administration.

References

1. Slater P. N., Biggar S. F., *J. Atmos. Oceanic Tech.*, 1996, **13**, 376-382.
2. Slater P. N., Biggar S. F., Holm R. G., Jackson R. D., Mao Y., Moran M. S., Palmer J. M., Yuan B., *Rem. Sens. Env.*, 1987, **22**, 11-37.
3. Biggar S. F., Dinguirard M. C., Gellman D. I., Henry P., Jackson R. D., Moran M. S., Slater P. N., *Proc. SPIE*, 1991, **1493**, 155-162.
4. Gellman D. I., Biggar S. F., Dinguirard M. C., Henry P. J., Moran M. S., Thome K. J., Slater P. N., *Proc. SPIE*, 1993, **1938**, 118-125.
5. Thome K., Markham B., Barker J., Slater J., Biggar S., *Photogramm. Eng. Remote Sensing*, 1997, **63**, 853-885.
6. Thome K. J., Gustafson-Bold C. L., Slater P. N., Farrand W. H., *Proc. SPIE*, 1996, **2821**.
7. Balick L. K., Golanics C. J., Shines J. E., Biggar S. F., Slater P. N., *Proc. SPIE*, 1991, **1493**, 215-223.
8. Gellman D. I., Biggar S. F., Slater P. N., Bruegge C. J., *Proc. SPIE*, 1991, **1493**.
9. Biggar S. F., Gellman D. I., Slater P. N., *Rem. Sens. Env.*, 1990, **32**, 91-101.
10. King M. D., Byrne D. M., Herman B. M., Reagan J. A., *J. Atmos. Sci.*, 1978, **35**, 2153-2167.
11. Flittner D. E., Herman B. M., Thome K. J., Simpson J. M., Reagan J. A., *J. Atmos. Sci.*, 1993, **50**, 1113-1121.
12. Thome K. J., Herman B. M., Reagan J. A., *J. Appl. Met.*, 1992, **31**, 157-165.
13. Biggar S. F., Labed J., Santer R. P., Slater P. N., Jackson R. D., Moran M. S., *Proc. SPIE*, 1988, **924**, 232-240.
14. Biggar S. F., Slater P. N., Gellman D. I., *Rem. Sens. Env.*, 1994, **48**, 242-252.